

Effect of Aluminum Siting in H-ZSM-5 on Reaction Barriers

Ashley T. Smith[§], Philipp N. Plessow^{§,*}, Felix Studt^{§,#}

[§] Institute of Catalysis Research and Technology, Karlsruhe Institute of Technology, Hermann-von-Helmholtz-Platz 1, D-76344 Eggenstein-Leopoldshafen, Germany.

[#] Institute for Chemical Technology and Polymer Chemistry, Karlsruhe Institute of Technology, Karlsruhe 76131, Germany

H-ZSM-5, methanol-to-olefin reaction • zeolites • reaction mechanisms • density functional theory • catalysis

ABSTRACT: We investigate the influence of acidity and confinement for different aluminum T-site substitutions in H-ZSM-5 using reactions related to the methanol-to-olefin (MTO) process as examples. We use density functional theory at the PBE-D3 level to study all 12 different T-sites existing in the MFI framework. We find that transition state energies vary by about 20 kJ/mol with the commonly employed T12 site having one of the lowest barriers. A large part of the energetic differences can be ascribed to differences in dispersion forces at the various surroundings of the acid sites, as also evidenced by smaller and uncorrelated differences in calculated heats of adsorption of ammonia. Our analysis shows that taking the T12 site as a computational active site model will yield reaction barriers that are among the lowest of all T-sites available.

INTRODUCTION

Zeolites are acidic microporous materials that are commonly employed as catalysts in the (petro)-chemical industry.¹⁻³ There is a large variety of zeolites, differing both in acidity and the microporous structure and thus the confinement of the active site where catalysis takes place. The acidity is introduced by substitution of a silicon atom of the zeolite framework with an aluminum atom, with the charge difference being compensated by a proton. Often, there are several tetrahedral sites (T sites) of the framework where substitution can take place, e.g. H-ZSM-5, the most commonly employed zeolite with MFI topology, has twelve different T sites (see Figure 1). These sites all differ in acidity and confinement with some not being accessible by (larger) reactants rendering them inactive. It is therefore conceivable that the overall activity of H-ZSM-5 is given by the sum of reactions occurring on all these different acid sites. While this has implications for the preparation⁴⁻⁵ and characterization⁶ of H-ZSM-5, it also potentially complicates computational modeling and the investigation of reaction mechanisms.

Computational modeling, mostly based on density functional theory (DFT), has become an integral part of mechanistic studies shedding light on how an acid site and its confinement facilitates specific reactions at the atomic level.⁷⁻⁸ Furthermore, with DFT, reaction barriers can be computed, allowing the search for rate-determining steps and the construction of kinetic models. Obviously, the outcome of these computational studies depends on the limitations of DFT and the accuracy with which free energies are obtained,⁷⁻¹¹ but also on the structural model of the active site employed in the calculations.¹²⁻¹⁷

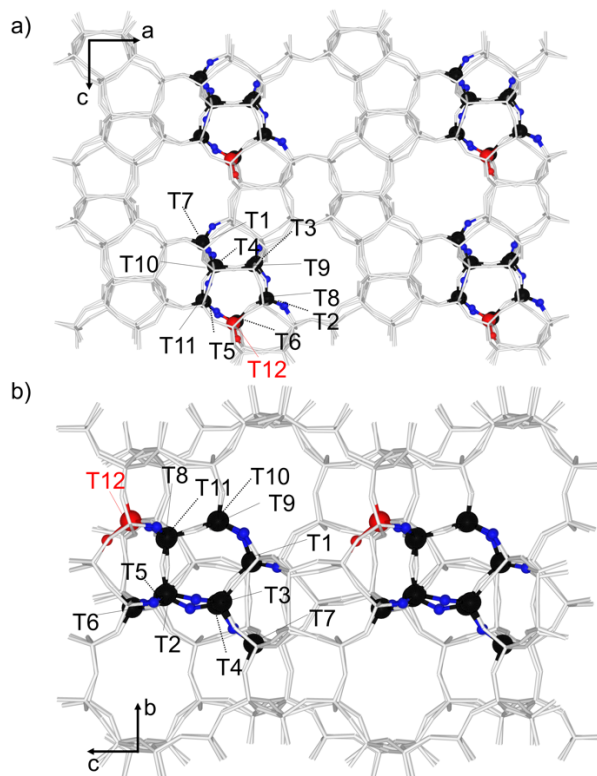


Figure 1. Location of the twelve different T-sites in H-ZSM-5 (MFI topology) shown in the direction of (a) the straight and (b) the sinusoidal channel. The T-12 site commonly used in computational models is highlighted in red.

Nowadays, it has become the standard to use periodic DFT calculations and functionals that account for dispersion

forces, which allows to model the entire zeolite pore such that the confinement of the zeolite is taken explicitly into account. The main approximations concerning the structural models of the acid site are (1) high Si/Al ratios (typically one isolated acid site per unit cell) and (2) specific locations of the aluminum substitution, e.g. in H-ZSM-5 it has become the standard approach to calculate reaction mechanisms using substitution at the T12 site (see Figure 1),¹⁸⁻²⁵ with only few exceptions.^{12-13, 16, 26-27} The influence of other choices of T sites on the calculated activity of H-ZSM-5 has been explored to a lesser extent. One example is given by the recent work of Grabow and co-workers who calculated the reaction mechanism of dimethyl ether (DME) synthesis for structural models of four of the twelve T-sites in H-ZSM-5.¹²⁻¹³

Herein, we use DFT at the PBE-D3 level to calculate the reaction barriers of five reactions related to the methanol-to-olefins (MTO) process over all twelve T-sites of H-ZSM-5. Our study considers an isolated Al substitution and thus a Si/Al ratio of 95:1. We investigate how these sites differ in terms of reaction barrier heights and transition state geometries and discuss how this is influenced by acidity and confinement.

METHODS

DFT calculation were performed in a similar manner as in our previous work.²⁵ We used the VASP program package in version 5.4.1 with the standard VASP-PAW potentials.²⁸⁻²⁹ The PBE density functional with Grimme's D3 dispersion correction (zero damping) has been employed (PBE-D3).³⁰⁻³¹ The Brillouin zone was sampled at the Γ point. Gaussian smearing with a width of 0.1 eV was used. The cutoff energy for the plane waves was 400 eV, while 800 eV has been used for the optimization of the lattice parameters. The optimized lengths of the lattice vectors of the unit cell of H-ZSM-5 are 20.340, 19.988 and 13.492 Å, as also used in earlier theoretical studies.²⁵ All structures have been fully relaxed and the convergence criteria for SCF cycles and geometry optimization were 10^{-8} eV and 0.01 eV/Å, respectively. The transition states were optimized using automated relaxed potential energy surface scans (ARPESS).³² Harmonic force constants were computed from a central finite difference method where the oxygen at which the reaction occurs as well as the adjacent T-atoms were included. All transition states were verified to contain only a single imaginary frequency corresponding to the transition vector of the reaction. In addition, the connectivity of transition states was confirmed through small displacement along the transition vector followed by optimization to the corresponding minima. In order to identify the strongest binding sites for adsorption and the lowest energy transition states, different proton locations at the four oxygen atoms surrounding alumina have been explored for the corresponding calculations (for a detailed discussion, see SI section S1).

RESULTS AND DISCUSSION

The five reactions investigated in this work are shown in Figure 2. All reactions relate to the MTO process. The first

reaction is the formation of a surface methoxy species (SMS) by reaction of methanol with the acid site. This reaction also constitutes the first step of the dissociative mechanism of DME synthesis. The four other reactions are methylation of ethene (2), propene (3), n-butene (4) and benzene (5) via the SMS, and thus probe the influence of confinement in the vicinity of the corresponding acid site. We note that the reported transition states only constitute the methylation steps, while additional, generally lower barriers are required for the rearrangement of adsorbates before and after methylation.^{27, 33} We also note that we only study the stepwise (dissociative) methylation mechanism, while the direct (associative) mechanism is known to be more favorable at lower temperatures for entropic reasons.³⁴⁻³⁶ The focus of this study is to shed light on the variations in adsorption energies and activation barriers arising from the choice of the employed acid site in the computational models. The comparison with experiments is difficult for two reasons. Firstly, the exact acid site distribution within the framework of H-ZSM-5 catalysts is unclear for the vast majority of experimental studies, as is the question which of these sites contribute most to the experimentally measured reaction rates. Secondly, the comparison of calculated and experimentally measured enthalpy barriers of this complex reaction network is for the most part not straightforward and comparison typically requires the involvement of microkinetic models of the specific reaction step that one wants to compare but also requires highly accurate ab initio methods, GGA-functionals are generally insufficient.^{23, 36}

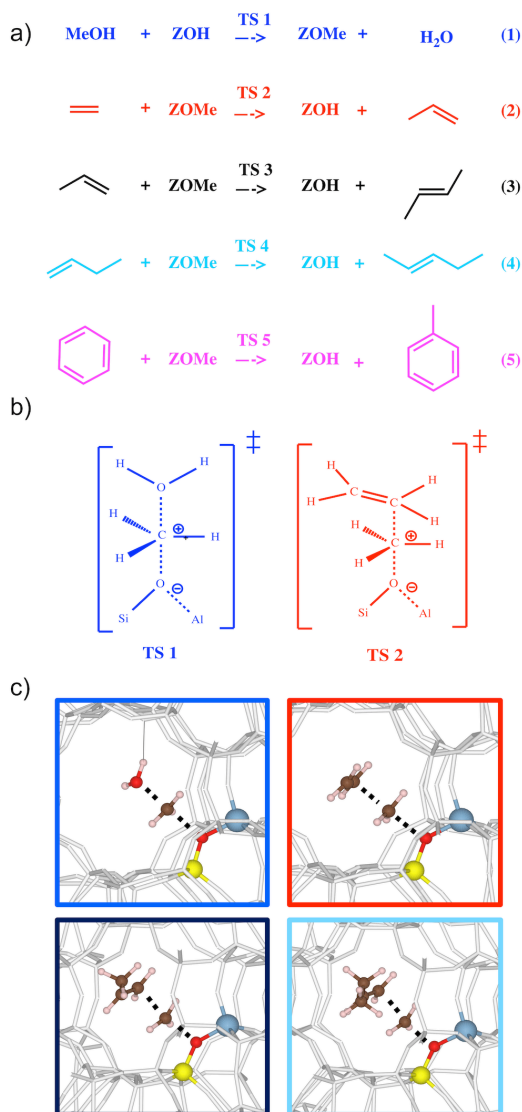


Figure 2. (a) The five reactions investigated herein. Note that the same color code is used throughout. (b) Schematic representation of the transition states for SMS formation and ethene methylation by SMS. (c) Calculated transition state geometries of reactions (1), (2), (3) and (4) at the T12 site of H-ZSM-5 (H, white; Si, yellow; Al, light blue; O, red; C, brown).

We start by evaluating the stability of the aluminum substitution relative to that using the T12 site (see also table S1 in the SI). In agreement with earlier theoretical studies,¹²⁻¹³ aluminum substitution of the T12 site is energetically favorable, only the T8 substitution is calculated to be slightly more preferred (-0.6 kJ/mol). Most other substitutions are 5-10 kJ/mol less stable. The favorable stability along with the accessibility of the T12 location at the intersection of the two channels is the reason why the majority of computational studies of H-ZSM-5 are based on the T12 site. The oxygen sites for the investigation of the reactivity were chosen based on stability and accessibility (see SI for detailed discussion).

One factor determining the reactivity of acidic zeolites is the strength in Brønsted acidity. One measure of this is

given by the ammonia heat of adsorption that can be conveniently calculated with DFT.³⁷⁻⁴⁰ Experimentally, it was found that the ammonia heat of adsorption does not vary significantly in H-ZSM-5 being on average -145 kJ/mol.⁴¹ This compares rather well with our calculated adsorption energies for the twelve T-sites that are in the narrow window of 138 to 160 kJ/mol (see Table 1) with an average of value of -148 kJ/mol (-149 kJ/mol for the T12 site), also in line with DFT calculations of Grabow and co-workers.¹²

Table 1. Overview of the calculated ammonia adsorption energies and reaction barriers. All barriers are given relative to the empty zeolite or SMS, respectively, and the reactants in the gas-phase. All values in kJ/mol, the T12 site is highlighted in bold.

T-site	ΔE_{NH_3}	Reaction barrier ΔE^\ddagger				
		(1)	(2)	(3)	(4)	(5)
1	-138	27	50	17	4	11
2	-138	26	49	19	2	16
3	-142	10	37	9	-3	14
4	-160	8	33	0	-6	32
5	-144	12	31	2	-14	0
6	-150	23	37	4	-9	5
7	-159	10	36	9	-2	37
8	-145	32	50	18	8	16
9	-149	22	26	-2	-11	17
10	-144	26	44	11	-3	4
11	-147	26	37	8	-7	0
12	-148	20	34	9	-8	10

The results of the calculations of transition state energies of the five reaction barriers over all twelve T-sites are given in Table 1. The calculated values agree rather well with computed values in the literature. For example, we calculated SMS formation at the T12 site to 20 kJ/mol relative to methanol in the gas-phase and the empty zeolite. Other DFT calculations for the same reaction range from 5 to 38 kJ/mol, depending on the functional used.^{25, 42-44} Grabow et al calculated the same reaction also for the T3, T10, and T11 sites, and found values of 1, 0, and -9 kJ/mol, respectively, thus being consistently lower.¹²⁻¹³ We attribute this to the use of a different functional. The value of 26 kJ/mol, which we obtain for the T11 site compares well with the 31 kJ/mol reported by Hibbitts and coworkers.²⁷

When comparing our data for the methylation of ethene, propene and n-butene, we observe that there is a general decrease of methylation barriers by about 30 kJ/mol and 40 kJ/mol for propene and butene methylation, respectively, when compared to that of ethene, and with all transition states referenced to an SMS and the olefin in the gas-phase. Similar trends have been observed for other zeolites, e.g. H-SSZ-13^{25, 38, 45} and have been attributed to the increased

stabilization of the cations as well as increases in vdW interactions with the zeolite.

This is also evident from Figure 3 that compares the transition state energies of propene and butene methylation with those of ethene. As can be seen, there is a general correlation between ethene and propene as well as n-butene methylation. Mean absolute deviations from the linear regression presented in Figure 3 are 1.8 and 2.5 kJ/mol for propene and n-butene methylation, respectively.

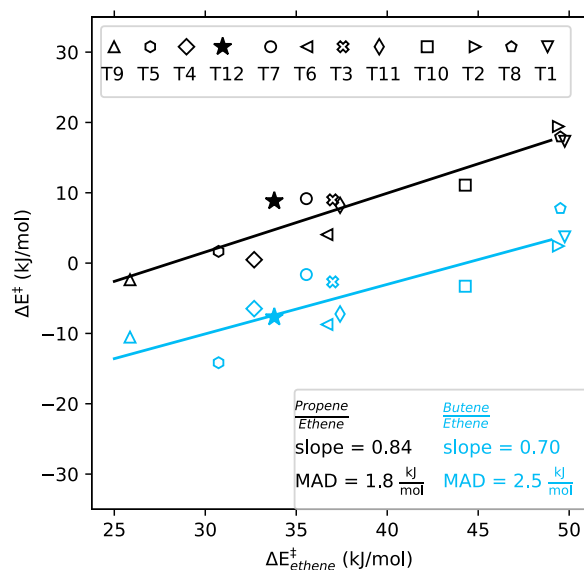


Figure 3. Transition state energies of propene (black) and n-butene (light blue) methylation via a SMS compared to that of ethene. All transition states are referenced to the SMS and the olefin in the gas-phase (see also Table 1). The filled data points indicate calculations for the T12 site of H-ZSM-5 which is highlighted in red in Figure 1.

Obviously, the reaction barriers employing the T12 site model are at the lower end of the spectrum of calculated values compared to other T-sites, with only T5 and T9 leading consistently to lower barriers. Comparing the three methylation reactions over the twelve T-sites of H-ZSM-5 reveals that the transition state energies vary by about 20 kJ/mol. For example, ethene methylation has the lowest transition state energy for the T9-site (26 kJ/mol) and the highest for the T1-site (50 kJ/mol), while this value is 34 kJ/mol for the commonly used T12-site.

Figure 4 shows how all five reaction barriers considered herein differ from that calculated for the T12 site. Generally, differences are less pronounced for smaller transition state geometries, e.g. SMS formation, and are largest for that of benzene methylation. The transition state energy of benzene methylation is particularly high for the T4 and T7 sites. We ascribe this to an increased steric repulsion due to the location of these acid sites, which are less accessible with parts of the benzene being as close as 3.2 Å to the framework atoms (see Figure 4). This is also evident from the PBE energy (PBE part of PBE-D3, see also Figure 5),

which contains the steric repulsion. The data shown in Figs. 4 and 5 is also listed in Tables S6 and S7.

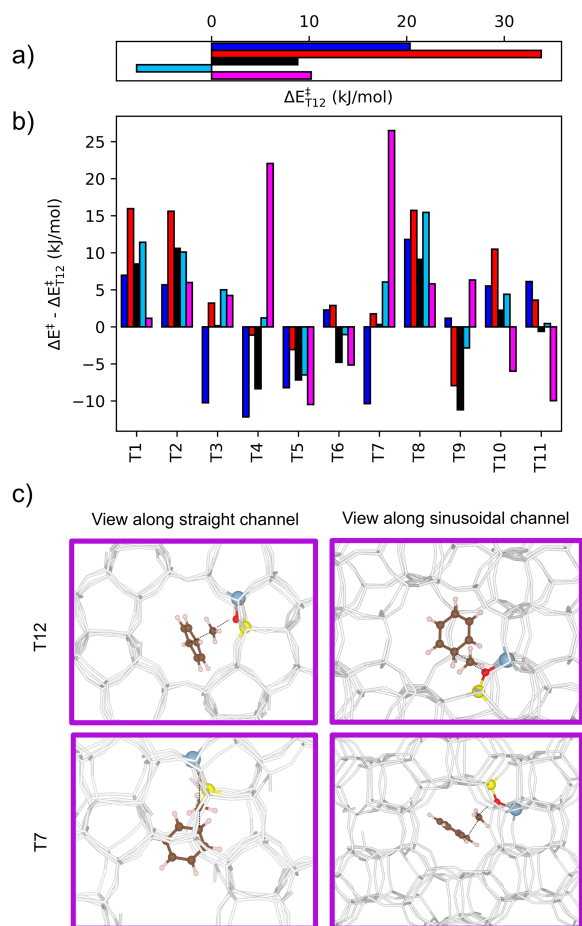


Figure 4. a) Transition state energies of reactions (1) to (5) calculated for the T12 site. b) Differences in transition state energies of reactions (1) to (5) relative to the T12 site. c) Optimized geometries of the transition states of benzene methylation occurring at the T12 and T7 sites viewed both along the straight and sinusoidal channels. Color code same as in Figure 2.

Figure 5 divides the energy contribution of the transition state energies into the PBE part that is derived from the solution of the Kohn-Sham equations and the dispersion part (D3) that is only a simple function of the position of the nuclei. These contributions are shown relative to those calculated for the T12 site. The transition state for SMS formation (reaction 1) at the T12 site has a PBE energy of 58 kJ/mol and contributions from vdW forces of -38 kJ/mol (see Figure 5a), resulting in an overall barrier height of 20 kJ/mol relative to methanol in the gas phase (see also Table 1). Interestingly, the PBE parts of the methylation barriers (ethene to benzene, reactions (2) to (5)) at the T12-site are all fairly similar, with values between 73 kJ/mol (propene) and 88 kJ/mol (benzene). The major differences observed for the T12 site are thus due to the increase in vdW interactions, linearly increasing from ethene (-44 kJ/mol), over propene (-73 kJ/mol), to 1-butene (-84 kJ/mol), with

benzene being similar to 1-butene (-77 kJ/mol). This is in line with earlier observations that the vdW interactions are a linear function of the numbers of atoms constituting the transition state.^{25, 42}

Figure 5b and Figure 5c show how the PBE and D3 parts differ for the various T-sites compared to that of T12. Interestingly, the differences in PBE energies ($\Delta\Delta E^\ddagger$ (PBE)) and dispersion interactions ($\Delta\Delta E^\ddagger$ (D3)) are comparable with MADs of 7.5 and 5.5 kJ/mol respectively. For most transition states they differ by less than 10 kJ/mol, with the exception of benzene methylation at T4 and T7 that we ascribe to steric hinderances (see discussion above). This is in line with the ammonia heat of adsorption (as a measure of acidity) that changes by a similar magnitude across the twelve T-sites (see Table 1). We hence conclude that the acidity and confinement effect of the acid site influence the transition state energy of a given reaction at the different T-sites in a similar manner. For bulky transition state geometries and less accessible acid sites, however, there can be highly repulsive interactions as evidenced for benzene methylation.

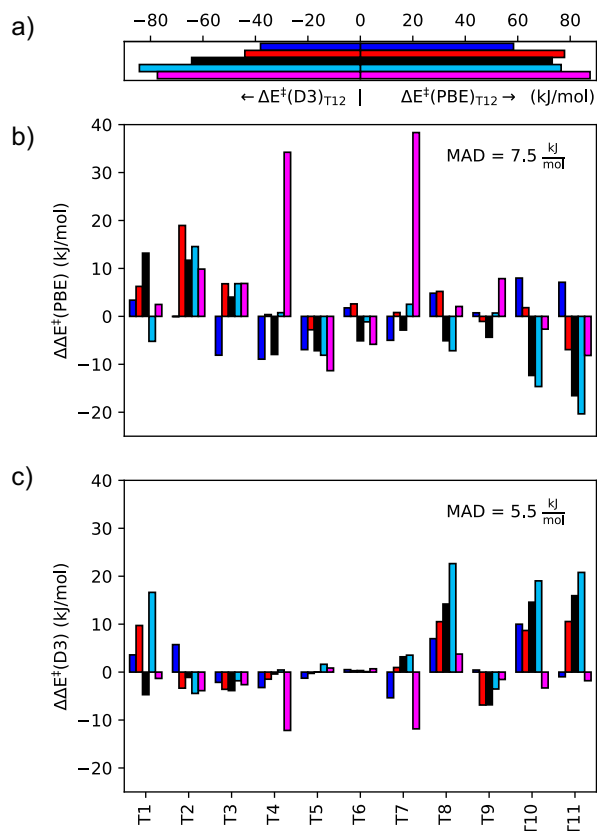


Figure 5. a) ΔE^\ddagger (PBE)_{T12} and ΔE^\ddagger (D3)_{T12} transition state energies of reactions (1) to (5) calculated for the T12 site. b) $\Delta\Delta E^\ddagger$ (PBE) energies of all other T-sites relative to those obtained for T12. c) $\Delta\Delta E^\ddagger$ (D3) energies of all other T-sites relative to those obtained for T12. Color code same as in Figure 2.

Our analysis so far only considered the transition state energies relative to the reactants in the gas-phase. Intrinsic barriers depend on the difference between the energy of the transition state and that of preadsorbed methanol. A comparison of intrinsic barriers and values for methanol adsorption are given in Table 2.

Table 2. Calculated adsorption energies for methanol and reaction barriers for SMS formation relative to gas-phase (ΔE_{app}^\ddagger) and adsorbed methanol (ΔE_{int}^\ddagger). All values in kJ/mol, the T12 site is highlighted in bold.

T-site	ΔE_{MeOH}	SMS formation barrier ΔE^\ddagger	
		ΔE_{app}^\ddagger	ΔE_{int}^\ddagger
1	-116	27	143
2	-116	26	142
3	-113	10	123
4	-123	8	131
5	-120	12	132
6	-121	23	143
7	-124	10	134
8	-117	32	149
9	-120	22	141
10	-123	26	149
11	-114	26	140
12	-124	20	144

Interestingly, the spread in adsorption energies of methanol is rather small with the T3 site having the weakest (-113 kJ/mol) and the T7 and T12 site having the strongest adsorption energies (-124 kJ/mol). The data is generally in good agreement with other values reported in the literature.^{34, 46-47} Transition state energies for SMS formation range from 8 to 32 kJ/mol and 123 to 149 kJ/mol for the apparent and intrinsic barriers, respectively, thus having similar spreads. This means that the choice of reference state (gas-phase vs adsorbed methanol) has only a small influence on the overall observed trends for SMS formation.

In order to analyze the influence of acid site location statistically, Figure 6 compares all energy barriers computed in this study to those obtained for the commonly used T12 site. Overall, we observe that roughly one third (35%) of the data consists of lower barrier and adsorption energies, while two thirds (65%) show higher energies. The overall mean absolute deviation (MAD) from the T12 site of 6.7 kJ/mol is rather small.

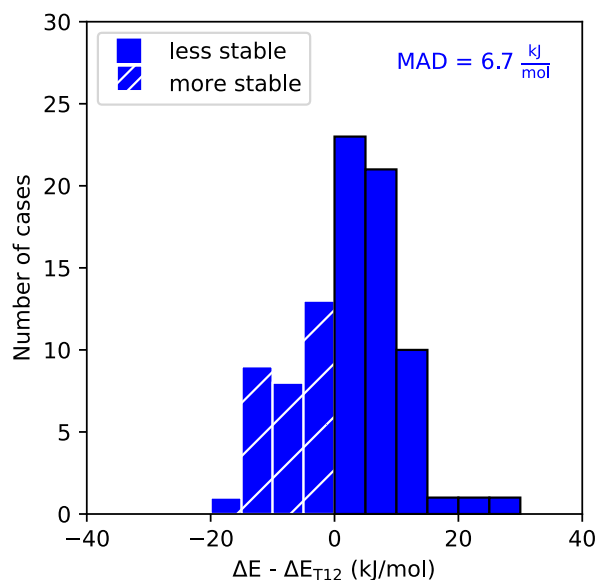


Figure 6. Statistics of the effect of alumina siting in H-ZSM-5, as measured relative to the adsorption energies and activation barriers calculated for the T₁₂ site for all data presented in this contribution. The width of the bars has been chosen as 5 kJ/mol.

SUMMARY AND CONCLUSIONS

We have investigated the influence of the acid site location in H-ZSM-5 on transition state energies of reactions related to the MTO process. We found that the energies of the transition states vary by about 20 kJ/mol with the commonly employed T₁₂ site having one of the lowest barriers. The energetic differences can be ascribed to both, differences in acid site acidity and dispersion forces at the various surroundings of the acid sites. While our analysis is based on the PBE-D₃ functional that severely underestimates reaction barriers related to the MTO process,¹⁰ we note that energy differences for the same type of transition state but different active sites are rather well described at this level of theory.⁴⁸ The current study does not include changes in entropy contributions, but those have been shown to vary only to a minor extent between different acid sites.^{12-13, 38}

This analysis thus reveals that taking the T₁₂ site as a computational model catalyst will give reaction barriers that are among the lowest of all T-sites available such that the T₁₂ model catalyst will capture the lowest transition states rather well if one assumes that all T-sites are present. This gives confidence in the commonly employed T₁₂-site model catalyst. However, one should also be aware that barriers can vary by 20 kJ/mol between the various T-sites, which translates to differences in rate constants of more than two orders of magnitude at relevant temperatures. While this study assumes a high Si/Al ratio and thus only one acid site per unit cell, we note that lower Si/Al ratios

will also influence transition state geometries and energies with a similar magnitude.¹⁵

ASSOCIATED CONTENT

Supporting Information

Additional analysis, total energies and Cartesian coordinates of all computed structures.

AUTHOR INFORMATION

Corresponding Author

*plessow@kit.edu

Author Contributions

The manuscript was written through contributions of all authors. / All authors have given approval to the final version of the manuscript.

ACKNOWLEDGMENT

The authors acknowledge support by the state of Baden-Württemberg through bwHPC (bwunicluster and JUSTUS, RV bw17D011). Financial support from the Helmholtz Association is also gratefully acknowledged.

REFERENCES

- Cheng, W.-C.; Habib Jr., E. T.; Rajagopalan, K.; Roberie, T. G.; Wormsbecher, R. F.; Ziebarth, M. S., Fluid Catalytic Cracking. In *Handbook of Heterogeneous Catalysis*, pp 2741-2778.
- Spivey, J. J., Review: Dehydration Catalysts for the Methanol/Dimethyl Ether Reaction. *Chem. Eng. Commun.* **2010**, *110* (1), 123-142.
- Stern, D. L.; Brown, S. H.; Beck, J. S., Isomerization and Transalkylation of Alkylaromatics. In *Handbook of Heterogeneous Catalysis*, pp 3168-3194.
- Dědeček, J.; Sobalík, Z.; Wichterlová, B., Siting and Distribution of Framework Aluminium Atoms in Silicon-Rich Zeolites and Impact on Catalysis. *Catalysis Reviews* **2012**, *54* (2), 135-223.
- Knott, B. C.; Nimlos, C. T.; Robichaud, D. J.; Nimlos, M. R.; Kim, S.; Gounder, R., Consideration of the Aluminum Distribution in Zeolites in Theoretical and Experimental Catalysis Research. *ACS Catal.* **2017**, *8* (2), 770-784.
- Sklenak, S.; Dedecek, J.; Li, C.; Wichterlova, B.; Gabova, V.; Sierka, M.; Sauer, J., Aluminium siting in the ZSM-5 framework by combination of high resolution ²⁷Al NMR and DFT/MM calculations. *Phys. Chem. Chem. Phys.* **2009**, *11* (8), 1237-47.
- Van Speybroeck, V.; De Wispelaere, K.; Van der Mynsbrugge, J.; Vandichel, M.; Hemelsoet, K.; Waroquier, M., First principle chemical kinetics in zeolites: the methanol-to-olefin process as a case study. *Chem. Soc. Rev.* **2014**, *43* (21), 7326-57.
- Van Speybroeck, V.; Hemelsoet, K.; Joos, L.; Waroquier, M.; Bell, R. G.; Catlow, C. R., Advances in theory and their application within the field of zeolite chemistry. *Chem. Soc. Rev.* **2015**, *44* (20), 7044-111.
- Studt, F., Grand Challenges in Computational Catalysis. *Frontiers in Catalysis* **2021**, *1*.
- Goncalves, T. J.; Plessow, P. N.; Studt, F., On the Accuracy of Density Functional Theory in Zeolite Catalysis. *ChemCatChem* **2019**, *11* (17), 4368-4376.

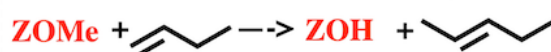
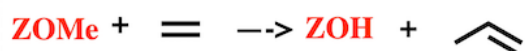
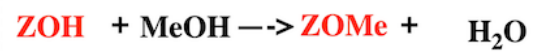
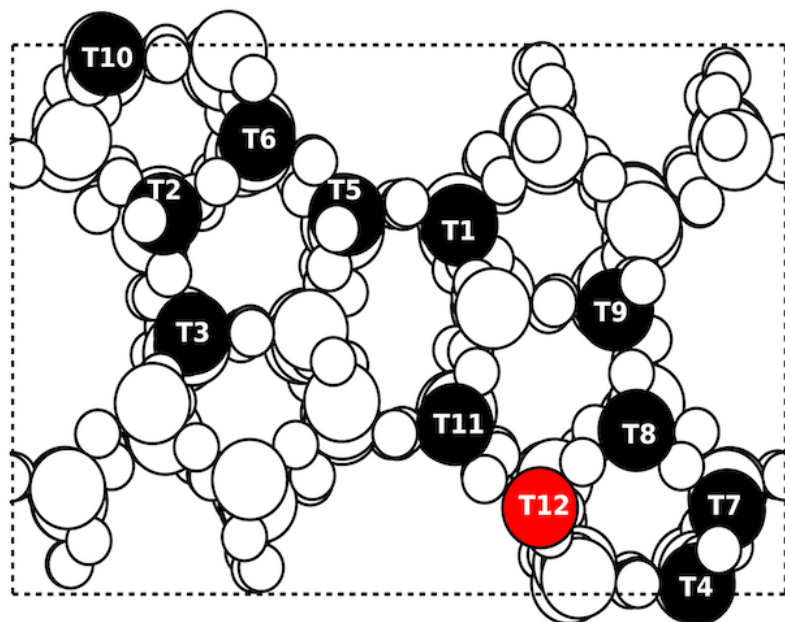
11. Sauer, J., Ab Initio Calculations for Molecule-Surface Interactions with Chemical Accuracy. *Acc. Chem. Res.* **2019**, *52* (12), 3502-3510.
12. Ghorbanpour, A.; Rimer, J. D.; Grabow, L. C., Periodic, vdW-corrected density functional theory investigation of the effect of Al siting in H-ZSM-5 on chemisorption properties and site-specific acidity. *Catal. Commun.* **2014**, *52*, 98-102.
13. Ghorbanpour, A.; Rimer, J. D.; Grabow, L. C., Computational Assessment of the Dominant Factors Governing the Mechanism of Methanol Dehydration over H-ZSM-5 with Heterogeneous Aluminum Distribution. *ACS Catal.* **2016**, *6* (4), 2287-2298.
14. Nystrom, S.; Hoffman, A.; Hibbitts, D., Tuning Brønsted Acid Strength by Altering Site Proximity in CHA Framework Zeolites. *ACS Catal.* **2018**, *8* (9), 7842-7860.
15. Hoffman, A. J.; Bates, J. S.; Di Iorio, J. R.; Nystrom, S. V.; Nimlos, C. T.; Gounder, R.; Hibbitts, D., Rigid Arrangements of Ionic Charge in Zeolite Frameworks Conferred by Specific Aluminum Distributions Preferentially Stabilize Alkanol Dehydration Transition States. *Angew. Chem. Int. Ed. Engl.* **2020**, *59* (42), 18686-18694.
16. Nimlos, C. T.; Hoffman, A. J.; Hur, Y. G.; Lee, B. J.; Di Iorio, J. R.; Hibbitts, D. D.; Gounder, R., Experimental and Theoretical Assessments of Aluminum Proximity in MFI Zeolites and Its Alteration by Organic and Inorganic Structure-Directing Agents. *Chem. Mater.* **2020**, *32* (21), 9277-9298.
17. Smith, A. T.; Plessow, P. N.; Studt, F., Trends in the Reactivity of Proximate Aluminum Sites in H-SSZ-13. *J. Phys. Chem. C* **2021**. DOI: 10.1021/acs.jpcc.1c03509.
18. Jones, A. J.; Carr, R. T.; Zones, S. I.; Iglesia, E., Acid strength and solvation in catalysis by MFI zeolites and effects of the identity, concentration and location of framework heteroatoms. *J. Catal.* **2014**, *312*, 58-68.
19. Nguyen, C. M.; Reyniers, M. F.; Marin, G. B., Theoretical study of the adsorption of C1-C4 primary alcohols in H-ZSM-5. *Phys. Chem. Chem. Phys.* **2010**, *12* (32), 9481-93.
20. Štich, I.; Gale, J. D.; Terakura, K.; Payne, M. C., Role of the Zeolitic Environment in Catalytic Activation of Methanol. *J. Am. Chem. Soc.* **1999**, *121* (14), 3292-3302.
21. Van der Mynsbrugge, J.; Hemelsoet, K.; Vandichel, M.; Waroquier, M.; Van Speybroeck, V., Efficient Approach for the Computational Study of Alcohol and Nitrile Adsorption in H-ZSM-5. *J. Phys. Chem. C* **2012**, *116* (9), 5499-5508.
22. Nguyen, C. M.; Reyniers, M.-F.; Marin, G. B., Theoretical Study of the Adsorption of the Butanol Isomers in H-ZSM-5. *J. Phys. Chem. C* **2011**, *115* (17), 8658-8669.
23. Svelle, S.; Tuma, C.; Rozanska, X.; Kerber, T.; Sauer, J., Quantum Chemical Modeling of Zeolite-Catalyzed Methylation Reactions: Toward Chemical Accuracy for Barriers. *J. Am. Chem. Soc.* **2009**, *131* (2), 816-25.
24. Lonsinger, S. R.; Chakraborty, A. K.; Theodorou, D. N.; Bell, A. T., The effects of local structural relaxation on aluminum siting within H-ZSM-5. *Catal. Lett.* **1991**, *11* (2), 209-217.
25. Plessow, P. N.; Studt, F., Theoretical Insights into the Effect of the Framework on the Initiation Mechanism of the MTO Process. *Catal. Lett.* **2018**, *148* (4), 1246-1253.
26. Alvarado-Swaigood, A. E.; Barr, M. K.; Hay, P. J.; Redondo, A., Ab initio quantum chemical calculations of aluminum substitution in zeolite ZSM-5. *The Journal of Physical Chemistry* **1991**, *95* (24), 10031-10036.
27. DeLuca, M.; Kravchenko, P.; Hoffman, A.; Hibbitts, D., Mechanism and Kinetics of Methylating C6-C12 Methylbenzenes with Methanol and Dimethyl Ether in H-MFI Zeolites. *ACS Catal.* **2019**, *9* (7), 6444-6460.
28. Kresse, G.; Furthmüller, J., Efficient Iterative Schemes for Ab Initio Total-Energy Calculations using a Plane-Wave Basis Set. *Phys. Rev. B* **1996**, *54* (16), 11169-11186.
29. Kresse, G.; Joubert, D., From Ultrasoft Pseudopotentials to the Projector Augmented-Wave Method. *Phys. Rev. B* **1999**, *59* (3), 1758-1775.
30. Perdew, J. P.; Burke, K.; Ernzerhof, M., Generalized Gradient Approximation Made Simple. *Phys. Rev. Lett.* **1997**, *78*, 1396-1396.
31. Grimme, S.; Antony, J.; Ehrlich, S.; Krieg, H., A Consistent and Accurate Ab Initio Parametrization of Density Functional Dispersion Correction (DFT-D) for the 94 Elements H-Pu. *J. Chem. Phys.* **2010**, *132* (15), 154104.
32. Plessow, P. N., Efficient Transition State Optimization of Periodic Structures through Automated Relaxed Potential Energy Surface Scans. *J. Chem. Theory Comput.* **2018**, *14* (2), 981-990.
33. Fečík, M.; Plessow, P. N.; Studt, F., A Systematic Study of Methylation from Benzene to Hexamethylbenzene in H-SSZ-13 Using Density Functional Theory and Ab Initio Calculations. *ACS Catal.* **2020**, *10* (15), 8916-8925.
34. Jones, A. J.; Iglesia, E., Kinetic, spectroscopic, and theoretical assessment of associative and dissociative methanol dehydration routes in zeolites. *Angew. Chem. Int. Ed. Engl.* **2014**, *53* (45), 12177-81.
35. Van der Mynsbrugge, J.; Visur, M.; Olsbye, U.; Beato, P.; Bjørgen, M.; Van Speybroeck, V.; Svelle, S., Methylation of benzene by methanol: Single-site kinetics over H-ZSM-5 and H-beta zeolite catalysts. *J. Catal.* **2012**, *292*, 201-212.
36. De Wispelaere, K.; Martínez-Espín, J. S.; Hoffmann, M. J.; Svelle, S.; Olsbye, U.; Bligaard, T., Understanding zeolite-catalyzed benzene methylation reactions by methanol and dimethyl ether at operating conditions from first principle microkinetic modeling and experiments. *Catal. Today* **2018**, *312*, 35-43.
37. Wang, C. M.; Brogaard, R. Y.; Weckhuysen, B. M.; Norskov, J. K.; Studt, F., Reactivity Descriptor in Solid Acid Catalysis: Predicting Turnover Frequencies for Propene Methylation in Zeotypes. *J. Phys. Chem. Lett.* **2014**, *5* (9), 1516-21.
38. Brogaard, R. Y.; Wang, C.-M.; Studt, F., Methanol-Alkene Reactions in Zeotype Acid Catalysts: Insights from a Descriptor-Based Approach and Microkinetic Modeling. *ACS Catal.* **2014**, *4* (12), 4504-4509.
39. Wang, C.-M.; Brogaard, R. Y.; Xie, Z.-K.; Studt, F., Transition-state scaling relations in zeolite catalysis: influence of framework topology and acid-site reactivity. *Catal. Sci. Technol.* **2015**, *5* (5), 2814-2820.
40. Liu, C.; Tranca, I.; van Santen, R. A.; Hensen, E. J. M.; Pidko, E. A., Scaling Relations for Acidity and Reactivity of Zeolites. *J. Phys. Chem. C* **2017**, *121* (42), 23520-23530.
41. Parrillo, D. J.; Lee, C.; Gorte, R. J., Heats of adsorption for ammonia and pyridine in H-ZSM-5: evidence for identical Brønsted-acid sites. *Appl. Catal., A* **1994**, *110* (1), 67-74.
42. Fečík, M.; Plessow, P. N.; Studt, F., Simple Scheme to Predict Transition-State Energies of Dehydration Reactions in Zeolites with Relevance to Biomass Conversion. *J. Phys. Chem. C* **2018**, *122* (40), 23062-23067.
43. Lesthaeghe, D.; Van der Mynsbrugge, J.; Vandichel, M.; Waroquier, M.; Van Speybroeck, V., Full Theoretical Cycle for both Ethene and Propene Formation during Methanol-to-Olefin Conversion in H-ZSM-5. *ChemCatChem* **2011**, *3* (1), 208-212.
44. Wen, Z.; Yang, D.; He, X.; Li, Y.; Zhu, X., Methylation of benzene with methanol over HZSM-11 and HZSM-5: A density functional theory study. *J. Mol. Catal. A: Chem.* **2016**, *424*, 351-357.
45. Wang, C.-M.; Wang, Y.-D.; Xie, Z.-K., Insights into the reaction mechanism of methanol-to-olefins conversion in HSAPO-34 from first principles: Are olefins themselves the dominating hydrocarbon pool species? *J. Catal.* **2013**, *301*, 8-19.
46. Costa, R. J.; Castro, E. A. S.; Politi, J. R. S.; Gargano, R.; Martins, J. B. L., Methanol, ethanol, propanol, and butanol

adsorption on H-ZSM-5 zeolite: an ONIOM study. *J. Mol. Model.* **2019**, *25* (2), 34.

47. Van der Mynsbrugge, J.; Moors, S. L. C.; De Wispelaere, K.; Van Speybroeck, V., Insight into the Formation and Reactivity of Framework-Bound Methoxide Species in H-ZSM-5 from Static and Dynamic Molecular Simulations. *ChemCatChem* **2014**, *6* (7), 1906-1918.

48. Plessow, P. N.; Studt, F., How Accurately Do Approximate Density Functionals Predict Trends in Acidic Zeolite Catalysis? *J. Phys. Chem. Lett.* **2020**, *11* (11), 4305-4310.

TOC



All 12 T-sites explored